Modeling and Control of Tissue Compression and Temperature for Automation in Robot-Assisted Surgery

Utkarsh Sinha[1], Baichun Li[2], and Ganesh Sankaranarayanan[3], *IEEE Member*

***Abstract*— Robotic surgery is being used widely due to its various benefits that includes reduced patient trauma and increased dexterity and ergonomics for the operating surgeon. Making the whole or part of the surgical procedure autonomous increases patient safety and will enable the robotic surgery platform to be used in telesurgery. In this work, an Electrosurgery procedure that involves tissue compression and application of heat such as the coaptic vessel closure has been automated. A MIMO nonlinear model characterizing the tissue stiffness and conductance under compression was feedback linearized and tuned PID controllers were used to control the system to achieve both the displacement and temperature constraints. A reference input for both the constraints were chosen as a ramp and hold trajectory which reflect the real constraints that exist in an actual surgical procedure. Our simulations showed that the controllers successfully tracked the reference trajectories with minimal deviation and in finite time horizon. The MIMO system with controllers developed in this work can be used to drive a surgical robot autonomously and perform electrosurgical procedures such as coaptic vessel closures.**

I. INTRODUCTION

Robotic surgery is becoming increasingly prevalent since it offers numerous benefits that include reduced patient trauma, shortened recovery time, increased dexterity, elimination of tremors, motion scaling, and increased ergonomics that reduces fatigue for the operating surgeon. Currently, robotic surgery is performed by an experienced surgeon by teleoperting the surgical robot to match his hand movements. Even though true teleoperation over long distance is possible, the operating surgeon is still situated in the same room. By automating either the full or part of the surgical procedure enables the surgeon to let the robot complete the tasks with greater precision and accuracy and eventually increase patient safety [1], [2]. Moreover with automation, forces and temeratures applied to the tissues can be precisely controlled. It also enables true long distance teleoperation with surgical robot.

Previous work on surgical automation has been focused on only tissue compression [3]–[6] or tissue retraction [7]. Apprenticeship learning techniques have also been used to automate two handed knot-tie procedures [8]. In this work, for the first time, we have modeled an electrosurgical procedure that involves both tissue manipulation and application of high frequency alternating current to heat the tissue to achieve tasks such as coaptic vessel closure, dissection, and coagulation.

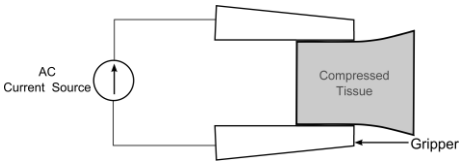

Figure 1. Electrosurgery on a block of tissue

Figure 1 provides a general overview of the environment for which our control system is being developed. A robotic gripper clamps down on a piece of tissue and applies AC current in order to desiccate it. Our goal is to develop a controller that can drive the gripper to compress the tissue to a desired thickness and then heat it up to the desiccation temperature. For the purposes of this project, the dynamics of the robot itself is being ignored since the primary concern is to control the gripper position and voltage.

II. SYSTEM MODELING

In order to automate the electrosurgical task, which is a nonlinear MIMO system with both tissue compression and heat constraints, it is broken down into three key components: tissue compression model, tissue impedance model, and tissue temperature model. Also, the following assumptions were made: movement of the mass is restricted to 1D and only resistive heating is modeled.

In the following sections we go through the process of creating each of these models and implementing feedback control for the electrosurgical task.

A. Tissue Compression Model

Soft tissues exhibit an exponential-like response when forces are applied to them [9]. Therefore we can model the tissue dynamics using a mass-spring-damper with a nonlinear spring (see Figure 2).

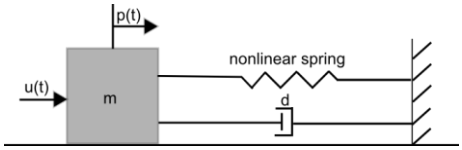

Figure 2. Mass-Spring-Damper Model

The nonlinearity of the spring in this model is given by

This work was supported by the RPI Office of Research Seed Grant

[1]U. Sinha is a co-terminal student in the Department of Electical and Computer Engineering, Rensselaer Polytechnic Institute, Troy, NY 12180, USA sinhau@rpi.edu

[2]Baichun Li, is a PHD candidate in the School of Mechanical Engineering and Automation, Northeastern University, Shenyang, Liaoning 110819, PRC baichun_li@hotmail.com

[3]G. Sankaranarayanan is a Research Assistant Professor in the Department of Mechanical, Aerosapce and Nuclear Engineering, Rensselaer Polytechnic Institute, Troy, NY 12180, USA sankag@rpi.edu

$$F_{spr} = \frac{s\alpha}{\beta+1}\left\{\left(1-\frac{p}{L_0}\right)e^{\beta\left(\left(1-\frac{p}{L_0}\right)^2-1\right)} - \frac{1}{\left(1-\frac{p}{L_0}\right)^2}e^{\beta\frac{p}{L_0-p}}\right\} \quad (1)$$

This model, called the Blatz-Ko model, was created by William L. Ko and P.J. Blatz for applications in finite elastic theory [10], [11]. The equation of motion for this system can now be written as

$$u = m\ddot{p} + d\dot{p} - \frac{s\alpha}{\beta+1}\left\{\left(1-\frac{p}{L_0}\right)e^{\beta\left(\left(1-\frac{p}{L_0}\right)^2-1\right)} - \frac{1}{\left(1-\frac{p}{L_0}\right)^2}e^{\beta\frac{p}{L_0-p}}\right\} \quad (2)$$

Where s is the contact surface area between one side of gripper and tissue, u is the force applied to the tissue, p is the position of the the robotic gripper, m is the mass of the tissue, d is the damping coefficient of the tissue, α and β are parameters related to the stiffness of the tissue and L_0 is the initial thickness if the tissue.

By choosing $x_1 = p$ and $x_2 = \dot{p}$, we can rewrite Equation 2 in the state-space form as

$$\dot{\mathbf{x}} = \begin{Bmatrix} x_2 \\ -\frac{d}{m}x_2 + \frac{s\alpha}{m(\beta+1)}\left\{\left(1-\frac{x_1}{L_0}\right)e^{\beta\left(\left(1-\frac{x_1}{L_0}\right)^2-1\right)} - \frac{1}{\left(1-\frac{x_1}{L_0}\right)^2}e^{\beta\frac{x_1}{L_0-x_1}}\right\} \end{Bmatrix} + \begin{Bmatrix} 0 \\ \frac{1}{m} \end{Bmatrix} u_1 \quad (3)$$

$$y_1 = x_1$$

B. Tissue Impedance Model

The impedance of the tissue is characterized based on the results of research on the bioimpedance of soft tissue under compression [12]. The tissue impedance can be represented by a Cole-Cole model as shown in Figure 3, where R_{ext} represents the resistance of the extracellular fluid, R_{int} is the resistance of the intracellular fluid, and C_m or C_{mem} is the bulk capacitance of the cellular membranes. It is important to note that the values for each of these elements change nonlinearly with respect to the compression of the tissue.

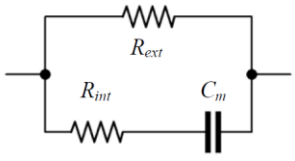

Figure 3. Fig. 3: Soft-Tissue Impedance Model

The overall impedance of the tissue can be written as

$$Z = \left\{\frac{1}{R_{ext}} + \frac{1}{R_{\text{int}} + \frac{1}{j\omega C_m}}\right\}^{-1} \quad (4)$$

In order to characterize the nonlinearity of R_{ext}, R_{int}, and C_{mem}, experimental data from [12] is used. Due to the lack of any mathematical equations corresponding to each circuit component, a nonlinear curve-fitting (as shown in Figure 4) is used to find the best-fit polynomial equations for the data presented in [12].

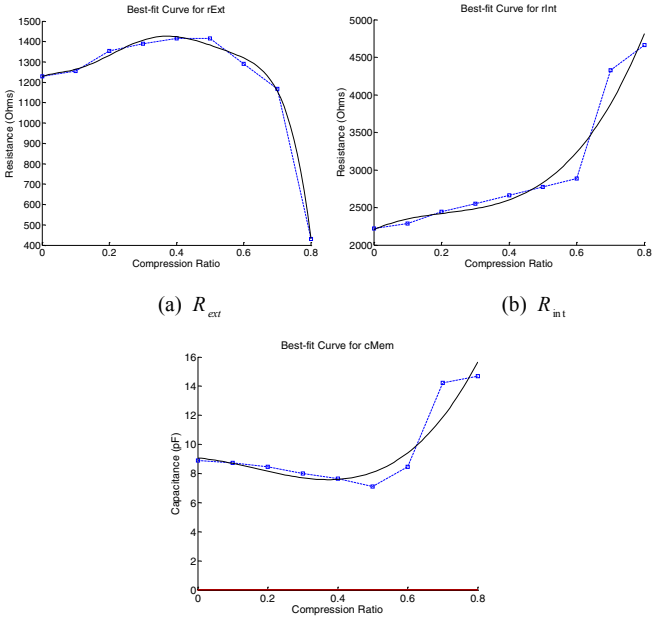

(a) R_{ext} (b) R_{int}

(c) C_{mem}

Figure 4. Best-fit curves for each component

The graphs above show the resistance/capacitance of each component with respect to compression ratio. Note that the maximum compression ratio in the plots above is limited to 0.8. This is due to the fact that at very high compression ratios, the tissue undergoes structural breakdown which affect its electrical properties. Moreover, due to the nonlinearity in the elasticity of the tissue, the amount of force needed to accomplish high compression ratio exceeds the capabilities of a surgical robotic grippers. Therefore, any data gathered for compression ratio above 0.8 is disregarded. The following polynomial equations are the best-fit curve for each component:

$$\begin{aligned} R_{ext} &= -171970\,x^6 + 339800\,x^5 - 243000\,x^4 \\ &\quad + 71810\,x^3 - 7450\,x^2 + 590\,x + 1230 \\ R_{\text{int}} &= 10203\,x^3 - 6559\,x^2 + 1980\,x + 2220 \\ C_{mem} &= \left(42.40\,x^3 - 21.06\,x^2 - 2.04\,x + 8.9\right)\times 10^{-12} \end{aligned} \quad (5)$$

Combining these equations together into Equation 4, over-all impedance as a function of tissue compression can be calculated when at an operating frequency of 200 KHz.

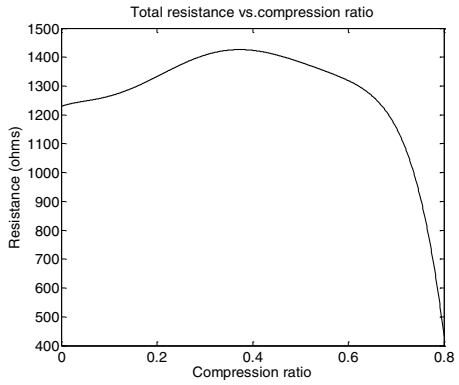

Figure 5. Soft-tissue resistance as a function of compression at standard electrosurgical frequency of 200 KHz

Figure 5 shows the variation in resistance (since we will be dealing with only real power in this work) as a function of tissue compression.

C. Tissue Temperature Model

The tissue temperature model characterizes the voltage-to-temperature map. With the impedance, Z, calculated in section II-B, the power dissipated in the tissue can now be written as $P = Re\left\{\frac{V^2}{Z}\right\}$, where V is the AC voltage applied to the tissue. For this work, we are assuming that the operating frequency is 200KHz, a commonly used frequency during electrosurgical procedures.

In order to fully characterize the temperature model, heat dissipation from tissue to air also needs to be taken into account. This is given by $q = h_c A_t \left|T - T_r\right|$, where q is change in energy per unit time, h_c is the heat transfer coefficient, A_t is the surface area subject to convection, T is the temperature of the object, and T_r is the ambient room temperature. Combining these equations, we can write the heat dissipated in the tissue as

$$\dot{Q} = P - q = V^2 Re\left\{\frac{1}{Z}\right\} - h_c A_t \left|T - T_r\right| \tag{6}$$

From this we can calculate the temperature change in the tissue as

$$\dot{T} = \frac{P - q}{mc} = \frac{V^2 Re\left\{\frac{1}{Z}\right\} - h_c A_t \left|T - T_r\right|}{mc} \tag{7}$$

Where m is the mass of the tissue and c is the specific heat capicity of the tissue. Choosing $x_3 = T$ and $u = V^2$, we can reformulate the temperature model in the following state-space form:

$$\dot{x}_3 = \frac{-h_c A_t \left|x_3 - T_r\right|}{mc} + \frac{Re\left\{\frac{1}{Z}\right\}}{mc} u_2 \tag{8}$$

$$y_2 = x_3$$

III. CONTROLLER DESIGN

The goal of this project is to design a controller that successfully tracks compression and temperature reference trajectories with minimal deviation and in finite time horizon.

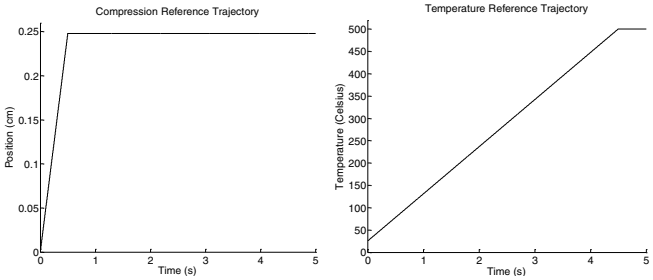

(a) (b)

Figure 6. (a) Compression Reference Trajectory Figure 6. (b)Temperature Reference Trajectory

Figure 6a shows a ramp-and-hold compression trajectory that would need to be tracked. The idea is that the robotic gripper would gradually compress the tissue to the desired thickness and then hold it there. In this case, we are assuming that the tissue's initial thickness is 0.0124m [11], so if the gripper successfully tracks the reference trajectory, it will have compressed the tissue by 20% after 0.5 seconds. These values are chosen to reflect realistic design constraints of the physical surgical instrument.

Similarly, Figure 6b demonstrates a ramp-and-hold temperature reference trajectory for the control system to track.

Once the electrosurgery process is completed, the robotic gripper can be fully opened and the voltage can go back to zero. Since this 'ramp-down' process doesn't need to be controlled, there is no need generate a reference trajectory for this part of the procedure.

In order to successfully accomplish reference tracking, a modular approach is taken when designing a controller, i.e. the tissue compression and tissue heat dissipation models are separately linearized and then PID controller is applied to each channel.

A. Linearization of Tissue Compression and Temperature Models

The tissue compression model defined in Equation 3 is a second order nonlinear system with a relative degree of 2. Thus, it has no zero dynamics and can be fully linearized. By applying the state feedback control law [13]

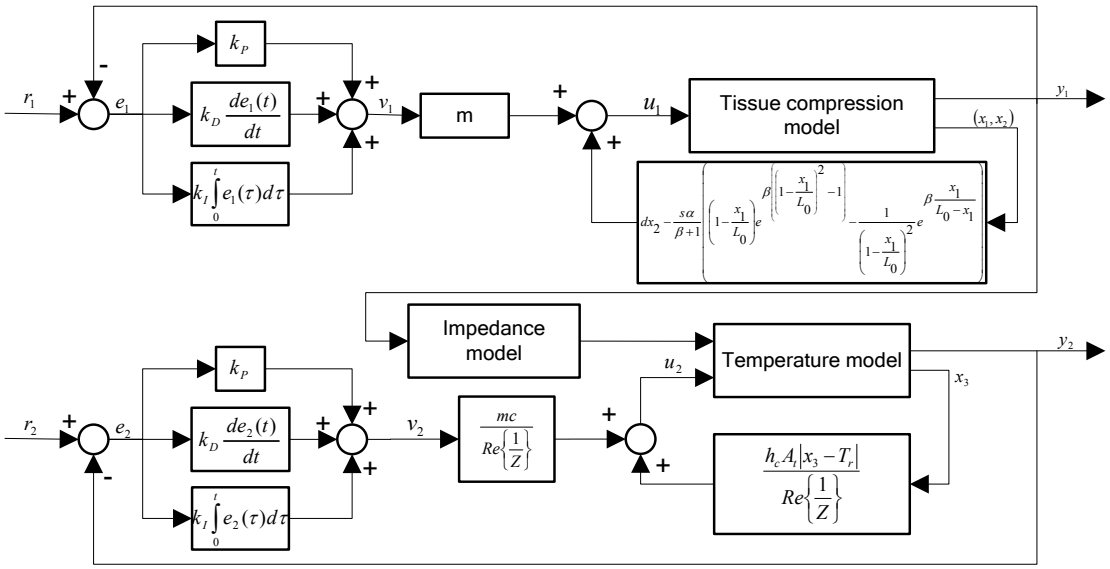

Figure 7. Control scheme of overall system

$$u_1 = \frac{v_1 - L_f^{\rho} h(x)}{L_g L_f^{\rho-1} h(x)} \tag{9}$$

Where f , g and h are state, input and output matrices, L_f and L_g represent Lie derivatives, and ρ is the relative degree, we get:

$$u_1 = mv_1 + dx_2 - \frac{s\alpha}{\beta+1}\left\{\left(1-\frac{x_1}{L_0}\right)e^{\beta\left(\left(1-\frac{x_1}{L_0}\right)^2-1\right)} - \frac{1}{\left(1-\frac{x_1}{L_0}\right)^2}e^{\beta\frac{x_1}{L_0-x_1}}\right\} \tag{10}$$

Similarly, the tissue temperature model defined in equation (10) is a first order nonlinear system with a relative degree of 1. Therefore, it has no zero dynamics and is fully linearizable. The feedback control law is applied once again to get:

$$u_2 = \frac{v_2 - L_f^{\rho} h(x)}{L_g L_f^{\rho-1} h(x)} = \frac{mc}{Re\left\{\frac{1}{Z}\right\}} v_2 + \frac{h_c A_t |x_3 - T_r|}{Re\left\{\frac{1}{Z}\right\}} \tag{11}$$

B. PID Controller

In order to track the reference trajectory for both the tissue compression and temperature, two separate PID controllers representing v_1 and v_2 in Equations 10 and 11 were defined as follows

$$v = k_P e + k_D \frac{de}{dt} + k_I \int_0^t e dt \tag{12}$$

Where e is the error between the desired and actual reference representing tissue compression and temperature. The control scheme is obtained, as shown in Figure 7. The r_1 is the compression reference trajectory, the r_2 is the temperature reference trajectory, the y_1 and y_2 are the compression position and temperature of the tissue .

IV. RESULTS

In order to track the reference trajectories, an exhaustive search was performed to fine tune the PID controllers whose values along with parameters used for testing is shown in Table I. A liver tissue was used as the target model whose parameters are provided in the Table I. The entire model with the controller was simulated in MATLAB.

TABLE I. PARAMETERS FOR MODELS AND THE CONTROLLERS

Symbol [units]		Value
Compression	k_P	15
	k_D	30
	k_I	0. 1
Temperature	k_P	40
	k_D	0.01
	k_I	0.3
d [N·s/m]		0.285 [14]
m [kg]		0.001302 [12]
s [m2]		7.15×10^{-5} [11]
α [Pa]		3289.4 [11]
β		20.63 [11]
L_0 [m]		0.0124 [12]
A_t [m2]		1.43×10^{-4} [11]
c [J/(kg·℃)]		3600 [15]
h_c [W/(m2·℃)]		10 [15]
T_r [℃]		25 [15]

The performance of this controller in tracking the compression reference trajectory is shown in Figure 8a. The system converges to the desired position with negligible deviation from the reference trajectory. Figure 8b shows the force applied to the tissue to achieve the desired compression.

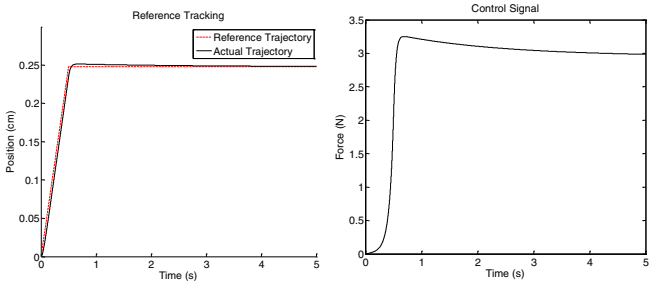

(a) (b)

Figure 8. (a) Compression reference tracking (b) Force applied to the tissue (Blatz-Ko model)

Figure 9a shows the results from tracking the temperature reference trajectory. It can be seen that the controller was able to track the reference with almost no deviation and it also converges to the desired temperature in finite time. Figure 9b shows the voltage applied to the tissue to achieve the desired temperature.

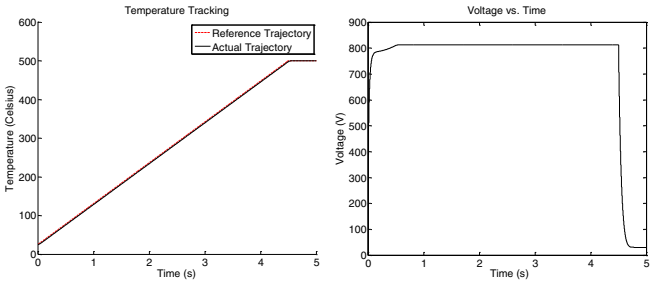

(a) (b)

Figure 9. (a) Temperature tracking using PID controller (b) Voltage trajectory applied to the tissue

V. CONCLUSION AND FUTURE WORK

In this work, a nonlinear MIMO model representing the variation of tissue compression and conductance under applied force was used to automate electrosurgical procedures such as coaptic vessel closure. The MIMO model with the two inputs being force and voltage and the two outputs being compression and temperature were separately linearized using state feedback linearization techniques. Two separate PID controllers were then used to track the ramp and hold reference trajectories. MATLAB simulation results showed that the controllers successfully tracked the trajectories with minimal deviation and in finite time horizon.

The next stage of this work will include optimal and model predictive control to satisfy both compression and temperature constraints. The thermal property of the tissue also needs to be modeled more accurately, and this would require in vivo experimentation on porcine. Moreover, in order to test the robustness of the system, the simulation needs to take sensor noise, disturbances, and other possible faults into account. In this work, the dynamics of the operating robot was not considered which will be part of our future work.

REFERENCES

[1] J. Bauer, B. R. Lee, D. Stoianovici, J. T. Bishoff, S. Micali, F. Micali, and L. R. Kavoussi, "Remote percutaneous renal access using a new automated telesurgical robotic system," Telemedicine Journal and E-Health, vol. 7, no. 4, pp. 341–346, 2001.

[2] H. Kang and J. T. Wen, "Robotic assistants aid surgeons during minimally invasive procedures," Engineering in Medicine and Biology Magazine, IEEE, vol. 20, no. 1, pp. 94–104, 2001.

[3] X. Yu, H. J. Chizeck, and B. Hannaford, "Comparison of transient performance in the control of soft tissue grasping," in Intelligent Robots and Systems, 2007. IROS 2007. IEEE/RSJ International Conference on, pp. 1809–1814, IEEE, 2007.

[4] X. Yu and H. J. Chizeck, "Equilibrium selection in automated surgery," in Biomedical Robotics and Biomechatronics, 2008. BioRob 2008. 2nd IEEE RAS & EMBS International Conference on, pp. 740–746, IEEE, 2008.

[5] X. Yu and H. J. Chizeck, "Lower bounds on the optimal control of soft tissue grasping," in Engineering in Medicine and Biology Society, 2008. EMBS 2008. 30th Annual International Conference of the IEEE, pp. 1943–1947, IEEE, 2008.

[6] G. Sankaranarayanan, V. S. Arikatla, and S. De, "A simulation framework for tool tissue interactions in robotic surgery.," Studies in health technology and informatics, vol. 173, pp. 440–444, 2011.

[7] S. Patil and R. Alterovitz, "Toward automated tissue retraction in robot-assisted surgery," in Robotics and Automation (ICRA), 2010 IEEE International Conference on, pp. 2088–2094, IEEE, 2010.

[8] J. Van Den Berg, S. Miller, D. Duckworth, H. Hu, A. Wan, X.-Y. Fu, K. Goldberg, and P. Abbeel, "Superhuman performance of surgical tasks by robots using iterative learning from human-guided demonstrations," in Robotics and Automation (ICRA), 2010 IEEE International Conference on, pp. 2074–2081, IEEE, 2010.

[9] Y. Fung, "Biomechanics: mechanical properties of living tissues. 1993."

[10] Farshad M, Barbezat M, Flüeler P, et al. Material characterization of the pig kidney in relation with the biomechanical analysis of renal trauma. Journal of Biomechanics, 1999, 32(4): 417-425.

[11] Rosen J, Brown J D, Sinanan M, et al. Biomechanical properties of abdominal organs in vivo and postmortem under compression loads. Journal of Biomechanical Engineering, 2008, 130(2): 021020.

[12] R. E. Dodde, Bioimpedance of soft tissue under compression and applications to electrosurgery. PhD thesis, The University of Michigan, 2011.

[13] H. K. Khalil, Nonlinear Systems. Prentice Hall, 1996.

[14] Kerdok A E. Characterizing the nonlinear mechanical response of liver to surgical manipulation. PhD Thesis. Harvard University Cambridge, MA, 2006.

[15] Mandel Y, Malki G, Adawi E, et al. Hemorrhage Control of Liver Injury by Short Electrical Pulses. PloS one, 2013, 8(1): e49852.